NANO: Brief Reports and Reviews
Vol. 3, No. 6 (2008) 449–454

World Scientific
www.worldscientific.com

MORPHOLOGY CONTROL OF CARBON NANOTUBES THROUGH FOCUSED ION BEAMS

M. LOYA, J. E. PARK, L. H. CHEN, K. S. BRAMMER,
P. R. BANDARU and S. JIN*
Materials Science and Engineering
University of California San Diego
La Jolla CA 92093-0411, USA
**jin@ucsd.edu*

Received 21 July 2008
Revised 29 September 2008

This research demonstrates the capability of controlled, focused ion beam (FIB)–assisted tailoring of morphologies in both multiwall carbon nanotubes (CNTs) and Y junction nonlinear CNT systems through defect engineering. We have shown that a 30 keV FIB Ga^+ ion beam at low ion milling currents of 1 pA can be used to partially reduce the CNT diameter, to provide electrical conduction bottleneck morphologies for linear CNTs, and to introduce both additive and subractive defects at Y junction locations of Y-CNT samples. Our aim is for this work to provide motivation for additional research to determine the effects of ion-beam-induced changes in modulating the physical and chemical properties of nanotubes.

Keywords: Carbon nanotubes; focused ion beam; defects; Y junction.

1. Introduction

There has been great interest in the electrical properties of carbon nanotubes (CNTs), as CNT-based molecular electronics offers significant potential as a nanoscale alternative to silicon-based devices.[1–6] For example, in a novel departure from linear CNT morphologies, we have shown recently that three-terminal CNT-based Y junctions can exhibit near-perfect and abrupt electrical switching, without the need for a separately fabricated gate.[7–13] An abrupt modulation of the current from an "on" to an "off" state, presumably mediated by defects and the topology of the junction, was observed in Y-shaped CNTs, synthesized in chemical vapor deposition (CVD) through the addition of Ti-based catalysts.[10]

It was seen during the examination of the CVD-synthesized Y junctions that while a few Y junction nanotubes have catalyst particles trapped at the junction region, the majority have no visible presence of extrinsic impurities. As we postulated[11] that defects could significantly affect the electrical transport and transistor-like behavior of the Y-CNTs, an ability to artificially introduce/control such defects and correlate with the electrical behavior is highly desirable. Furthermore, an ability to fabricate Y junction-based devices in intentionally arranged configurations (e.g. a periodic array at predictable positions) would be very desirable for eventual technical applications.

The first step toward these advances requires the creation/manipulation of defects at Y junctions for property modulation. It may also be possible[10] that heterogeneous nucleation of CNT branches on defect sites could be initiated at the sites of the defects, which would have enormous implications for the CNT-based interconnect. The defects can be either (i) *subtractive* or (ii) *additive*. In the former case, for example, nanoholes/nanonotches in

the CNT morphology can induce localized resistance changes for use in creating specific integrated circuits. Alternatively, as in (ii), one can *add* additional material to induce localized strains for affecting the CNT properties, or insert catalyst particles, say through localized catalyst (e.g. Fe, Co, or Ni) deposition, for subsequent CVD growth of periodic nanotube arrays. In this work, we aim to demonstrate the artificial introduction of such defects in CNTs for future investigation of their effect on the electrical properties of the manipulated nanotube morphologies.

One method of adding defects is through the use of focused ion beams (FIBs), which can be configured to carve out selective portions of the nanostructure, e.g. via ion milling for specific thicknesses. Alternatively, localized decomposition of an organometallic precursor, through ion beams,[14] can be used to induce precise metal deposition. Generally, such techniques are an extension of ion irradiation methods, traditionally used for modifying materials, e.g. in ion-implantation-based processing extensively used in semiconductor processing, where defects and controlled damage can be introduced. In this paper we report experimental results on FIB-induced additive (i.e. through depositing Pt–C islands on the junction) and subtractive (i.e. through CNT wall necking) defects in multiwalled CNTs and their effect on the electrical resistance.

In our experiments, FIB was also used to contact the CNTs, with good accuracy, for enabling four-point electrical resistance measurements, as illustrated in Fig. 1. We use a dual-beam FIB (Zeiss Cross Beam® Model 1540), where both electron and ion beams can be used for the creation of additive and subtractive defects in CNTs. While the electron beams impinge vertically [to minimize lens aberrations], the ion (Ga^+) column is oriented at angle 54°.

Nanostructuring using FIBs is governed by different parameters of the beam, such as ion dose and energy, as well as the inherent structural properties and potential chemical change as a result of ion milling. Optimal mill conditions for surface-sensitive specimens such as carbon nanotubes are challenging, in particular because beam size resolution during the mill process is greatly reduced under the surface imaging SEM mode and when low mill current FIB mode dual cross beams are performed in combination. In this research an extremely low current of 20 pA and the layered raster technique were necessary for delicate reduction of the wall

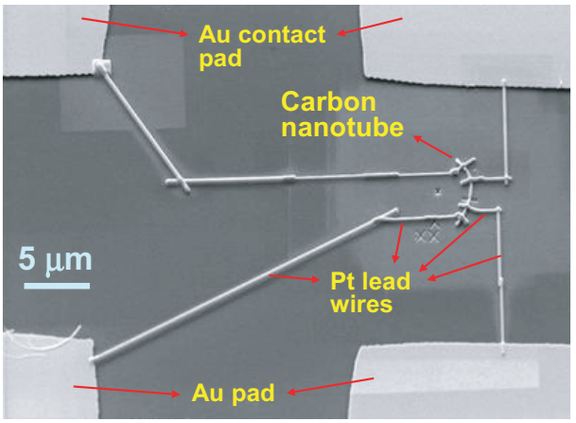

Fig. 1. Four-point measurement for a CNT sample on SiO_2 substrate using FIB-deposited Pt lead wires connected to surrounding, larger-area Au contact pads.

diameter of an individual CNT. The Pt lead wires were deposited in 1–2 μm segments $\sim$80 nm thick, using Ar as a precursor gas.

2. Results and Discussion

2.1. *Subtractive defect, through FIB-induced carving of MWNTs*

As traditional electron-beam-based lithography is complicated, time-consuming and costly, we have earlier demonstrated a unique, rapid and direct-write-based nanopatterning of the electrical contacts and interconnects to larger electrodes using the FIB-based metal deposition process.[14] In the current work, four-point electrical measurements using FIB-based electrical leads, to avoid the contact resistance problem,[15] will be illustrated. Such methods are especially suitable for short (<1 μm) CNTs. The multiwalled CNTs, in both the linear and Y junction shapes, were fabricated by CVD processes, as described previously.[10]

FIB-based metal deposition for electrical contact lines is arranged through a gas delivery system in conjunction with the ion beam to produce site-specific deposition of metals. The Pt electrical lead wires were deposited by ion-beam-assisted chemical vapor deposition using a Pt precursor $(CH_3)_3(CH_3C_5H_4)Pt$ known as methylcyclopentadienyl platinum trimethyl (melting point 30°C).

The controlled subsequent release of the metal can then be used to form metal lines/layers over the substrate. It should be noted that an associated disadvantage of FIB metal line deposition is that the metal is often contaminated (e.g. being a

mix of Pt and carbon), with relatively high, approximately increased tenfold electrical resistivity values of 160–200 $\mu\Omega$ cm (*cf.* pure Pt, which has a resitivity of $\sim$15 $\mu\Omega$ cm). We are working on annealing treatment in an effort to obtain improved metallic conductivity.

An example of FIB-metal-deposited lines to contact CNTs is shown in the low magnification scanning electron microscope (SEM) micrograph in Fig. 1. The outer lead wires were used for applying a current to the CNT sample, while the inner two leads were used for measuring the voltages, to obtain the I–V curves.

For this particular CNT, we employed the FIB milling process (using 30 keV Ga^+ ions) for carving out a portion of the nanotube, similar to what was reported previously,[16,17] but adding four-point probe lead patterns created by FIB-assisted deposition of Pt, where a controlled amount of the precursor gas $(CH_3)_3(CH_3C_5H_4)Pt$ is introduced through the inlet capillary positioned $\sim$100 μm above the sample surface.

Although it is uncommon to mill at such low current values, in the case of our nanoscale manipulation the mill current and imaging current required the lower limit values of the instrument of the 1 pA current for both milling and imaging. The reason that 1 pA current FIB milling will have fine targeted milling results (and deposition results under the 1 pA ion current imaging mode) is the command of designated areas where only the Ga^+ ion beam will strike the sample surface.

When one is using a gas source for metal deposition in FIB methods, the gas molecules are adsorbed on the surface in the vicinity of the gas inlet, but decompose only where the Ga^+ ion beam strikes. Repeated adsorption and decomposition result in the buildup of material in the Ga^+ ion scanned region. The ion-beam-assisted chemical-vapor-deposition process consists of a fine balance between sputtering and deposition; for example, if the primary beam current density is too high for the deposition region, then undesired milling will occur.[18]

Delicate ion milling currents in the range of 1 pA were applied on the CNT sample to etch the MWNT progressively, as shown in the higher magnification SEM micrograph (inset) of Fig. 2. The FIB conditions for etching and deposition were performed in mill for depth mode imaging current at the lowest current of the instrument of 1 pA, the mill current of 1 pA and the overall mill depth of 0.1 μm.

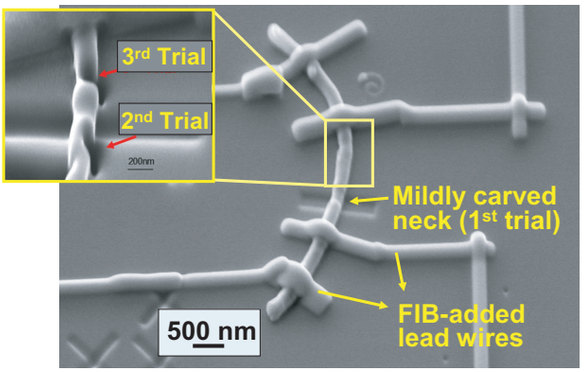

Fig. 2. Reduction in the cross-sectional area of the MWNT by FIB milling, followed by four-point electrical measurements (see Fig. 3).

We report here the four-point electrical measurements as a function of successive nanotube morphology modifications. Linear MWNTs exhibit metallic conduction and linear I–V curves, (Fig. 3), as expected. The initial resistance (R) was $\sim$7 KΩ. As the CNT sample cross-sectional area was successively reduced to 60% (marked "2nd Trial" in Fig. 2) and $\sim$ 10% (marked "3rd Trial"), the resistance was increased to 12 KΩ and $\sim$100 KΩ respectively, in close correspondence to the reduction in the cross-sectional area of the carved region. The results of these measurements, shown in Fig. 3(a), are a clear indication of the correlation between the increased electrical resistance and the reduced cross-sectional area.[19] The plot of electrical conductivity versus estimated cross-sectional area of the CNT altered by FIB sculpting is shown in Fig. 3(b); it displays a roughly linear relationship between the electrical conductance and the smallest CNT cross-sectional area (smallest-necked region).

Uniform bottleneck geometries resulted from the same milling recipe conditions. However, the beam raster was perpendicular to linear nanotube samples. The FIB conditions using the 30 keV Ga^+ ion beam rastered perpendicular to the length of the nanotube at a low current level of 1 pA and the 1 pA FIB imaging mode, as shown in Table 1, recipes which are the lower limit operational parameters for the 1540$\times$ cross beam machine for imaging and milling. As a consquence, we see in Fig. 4 the uniform symmetric milling results creating a bottleneck geometry along the ion-milled sample regions (such a thin necking of CNTs sometimes as narrow as $\sim$20 nm, was introduced, with repeatable results in this site-specific manner, as shown in Fig. 4). In addition, subtractive hole defects were created

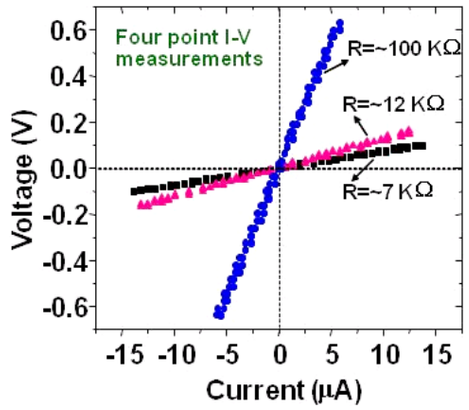

(a)

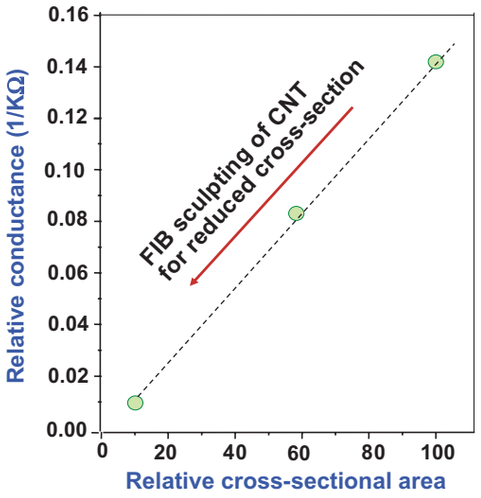

(b)

Fig. 3. (a) Four-point I–V measurement data for the MWNT sample shown in Figs. 1 and 2 after successive FIB millings to progressively reduce the cross-sectional area. (b) The relative conductance decreases with increased reduction in the cross-sectional area by the ion milling process.

Table 1. FIB milling and deposition conditions are pushed to the lower limit of the instrument.

Mill for depth mode	Value
Mill depth	0.1 μm
Layer raster	5
FIB imaging current	1 pA
FIB milling current	1 pA
SEM EHT	5 kV
FIB EHT	30 keV
FIB emission target	2.2 μA
Pt deposition with thickness	**Value**
Deposition thickness	0.1 μm
Layer raster	5
FIB imaging current	1 pA
FIB milling current	1 pA
SEM EHT	5 kV
FIB EHT	30 keV
FIB emission target	2.2 μA

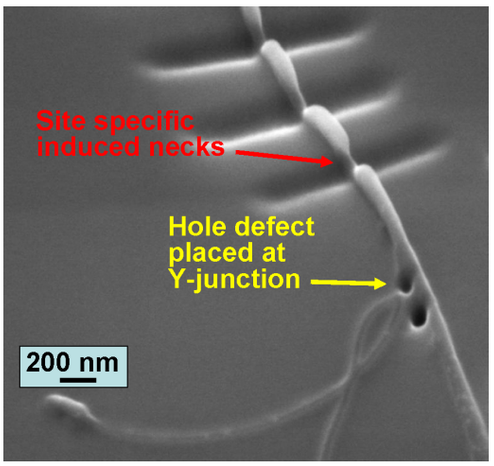

Fig. 4. SEM Image: FIB-induced necking defects on the MWNT length, and nanohole defects at Y junction sites (in the lower right part of the figure).

in a controlled manner at the Y junction (Fig. 5), which demonstrates a capability for partial or total removal of either nanostructure or extrinsic impurities inherent with Y junction CNTs.

The subtractive defect introduced with ion milling resulted in nanohole dimensions targeted near Y junction sites. These results offer interesting possibilities for defect nanoengineering; for example, the hole can be refilled with other material. As the bias voltage applied to the MWNT Y junction is quite large (in the 100 mV range),[11,20] it is expected that many walls of the MWNT will contribute to the electronic conduction. The presence of an *insulating/dielectric* foreign nanoparticle island and residual charge in the junction conduction paths will potentially blockade current flow, leading to an abrupt switching-off behavior of the current. On the other hand, the delocalization of the electrons over *metallic* material, introduced into the holes, can be seen as a size-dependent localized scattering center for modulating the electron transport characteristics.

Furthermore, it would be interesting to compare in detail the Y junction behavioral characteristics of semiconducting versus metallic versus dielectric nanoparticles inserted into the nanohole space. Such refilling of the nanohole with extrinsic

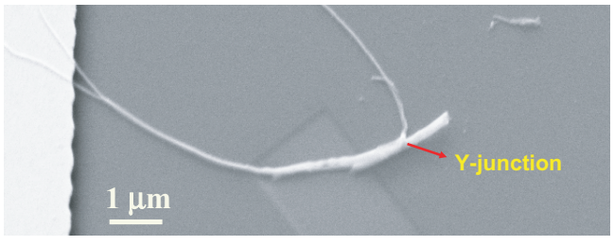

(a)

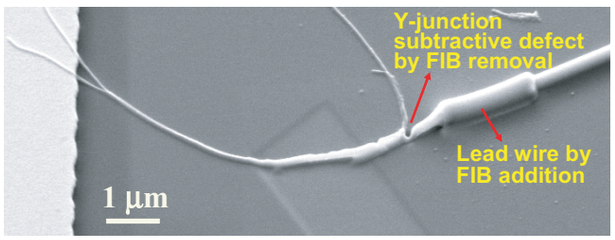

(b)

Fig. 5. (a,b) Subtractive defects introduced near the CNT Y junction. The Pt lead wire attachment to one of the branches (right side) of the Y junction nanotube is also depicted.

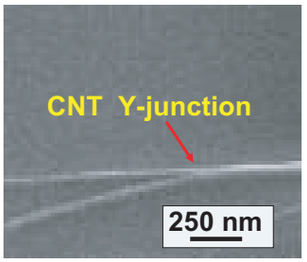

(a)

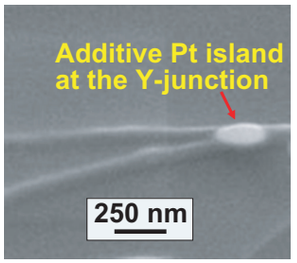

(b)

Fig. 6. Additive defects artificially introduced at the Y junction CNT location via the FIB Pt deposition mode. (a) Before (b) after island deposition at the junction site.

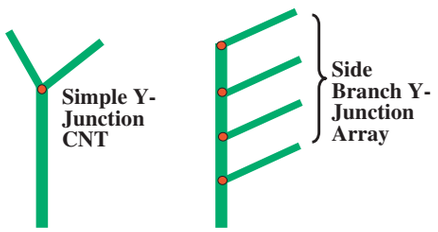

(a) (b)

Fig. 7. Schematic of the Y junction carbon nanotube: (a) a simple Y junction; (b) an array Y junction.

material can also be accomplished through the FIB-based metal deposition, or through the EBID (electron-beam-induced deposition) nanopatterning technique.[21] A postinsertion annealing heat treatment can also be applied to improve the particle–MWNT interface characteristics.

2.2. *Additive defects by FIB-induced metal deposition on MWNTs*

Our method of introducing site-specific additive defects was successful, and it shows a controlled process of addititive defects via FIB Pt deposition at the Y junction region of Y-CNT samples, as shown in Fig. 6. This method may be expanded for engineering branches on the linear nanotubes for creating highly desirable arrays of Y junction CNTs or interconnects. Such catalyst particles can affect the Y junction electronic properties, and the possible effect of the catalyst remnant at the Y junctions was discussed previously.[22] The extra CNT nucleating catalyst nanoparticles (such as Ni or Co) periodically placed along the length of the linear CNTs may be envisioned for preparation of periodic Y junction transistor arrays, as illustrated in Fig. 7.

It is known that in addition to the well-known nanotube nucleating catalyst metals Fe, Ni, Co and their alloys, Pt and Pd also serve as efficient catalysts for nucleation and growth of CNTs.[23–25] Potentially, these catalyst particles may also serve as seeds for CNT growth if the CVD is carried out in the presence of an electric field to guide the nanotube synthesis.[26,27] Such CNT growth would produce a periodic array of Y junctions, as illustrated in Fig. 7(b). The CNT nucleation and growth can follow either a base growth mechanism, as in Fig. 7(b), or a tip growth mechanism, in which the catalyst nanoparticles stay at the tip of growing/advancing CNTs. Such array fabrication is being planned/conducted for the future, and our preliminary studies, as reported here, will contribute to the CNT device applications with an array transistor configuration. In addition, the presence of these metal particles may contribute to nanoscale localized strains on the CNTs which may allow controlled modulation of their electronic conduction properties.

3. Summary

We have shown earlier that Y junction carbon nanotubes offer an exciting possibility of nanoscale, self-gated transistors with abrupt switching and logic capabilities. Motivation for this research is

to devise a method to artificially introduce such moieties in a controlled manner for architecting nano Y junction arrays. As the precise nature of the junction is thought to be crucial, in this paper we have introduced suitable modification techniques, using focused ion beams, to place subtractive/additive defects at the junction, through site-specific engineering.

We have demonstrated promising FIB milling and deposition conditions and techniques used for site-specific engineering at locations on linear CNTs as well as junctions of Y-CNTs, which can be useful for modification of structures and electrical transport properties of CNTs in general.

Acknowledgments

We acknowledge the support of this work from NSF-NIRTs under grant numbers DMI-0210559 and DMI-0303790, the ONR Grant (N00014-06-1-0234), the University of California Discovery Fund under grant number ele05-10241/Jin, and the Ministry of Commerce, Industry and Energy, Korea, through the next-generation microsystems packaging program. We would also like to thank the Zeiss laboratory at the University California, Irvine, and John Porter and Clive Hazelton for assistance and support, and Prof. Apparao Rao of Clemson University for supplying the carbon nanotube samples.

References

1. R. Martel, T. Schmidt, H. R. Shea, T. Hertel and P. Avouris, *Appl. Phys. Lett.* **73**, 2447 (1998).
2. S. J. Tans, A. R. M. Verschueren and C. Dekker, *Nature* **393**, 49 (1998).
3. A. Javey, J. Guo, Q. Wang, M. Lundstrom and H. Dai, *Nature* **424**, 654 (2003).
4. H. W. C. Postma, T. Teepen, Z. Yao, M. Grifoni and C. Dekker, *Science* **293**, 76 (2001).
5. Z. Yao, H. W. C. Postma, L. Balents and C. Dekker, *Nature* **402**, 273 (1999).
6. R. H. Baughman, A. A. Zakhidov and W. A. de Heer, *Science* **297**, 787 (2002).
7. A. N. Andriotis, M. Menon, D. Srivastava and L. Chernozatonski, *Phys. Rev. B* **65**, 165416 (2002).
8. D. Csontos and H. Q. Xu, *Phys. Rev. B* **67**, 235322 (2003).
9. A. N. Andriotis, D. Srivastava and M. Menon, *Appl. Phys. Lett.* **83**, 1674 (2003).
10. N. Gothard, C. Daraio, J. Gaillard, R. Zidan, S. Jin and A. M. Rao, *Nanolett.* **4**, 213 (2004).
11. P. R. Bandaru, C. Daraio, S. Jin and A. M. Rao, *Nature Mater.* **4**, 663 (2005).
12. J. Park, C. Daraio, S. Jin and P. R. Bandaru, J. Gaillard and A. M. Rao, *Appl. Phys. Lett.* **88**, 243113 (2006).
13. Y. C. Choi and W. Choi, *Carbon* **43**, 2737 (2005).
14. V. Gopal, V. R. Radmilovic, C. Daraio, S. Jin, P. Yang and E. A. Stach, *Nano Lett.* **4**, 2059 (2004).
15. S. Jin, J. E. Graebner, T. H. Tiefel and G. W. Kammlott, *Appl. Phys. Lett.* **56**, 186 (1990).
16. B. Q. Wei, J. D'Arcy-Gall, P. M. Ajayan and G. Ramanth, *Appl. Phys. Lett.* **83**, 3581 (2003).
17. A. V. Krasheninnikov and F. Banhart, *Nature Mater.* **6**, 723 (2007).
18. L. A. Gianunuzzi and F. A. Stevie, *Introduction to Focused Ion Beams* (Springer, New York, 2005).
19. Yuzvinsky *et al.*, *Nano Lett.* **6**, 2718 (2006).
20. P. G. Collins, M. Hersam, M. Arnold, R. Martel and P. Avouris, *Phys. Rev. Lett.* **86**, 3128 (2001).
21. I. C. Chen, L. H. Chen, X. R. Ye, C. Daraio, S. Jin, C. A. Orme, A. Quist and R. Lal, *Appl. Phys. Lett.* **88**, 153102 (2006).
22. A. N. Andriotis, M. Menon and D. Srivastava, *Appl. Phys. Lett.* **79**, 266 (2001).
23. D. Lupu, A. R. Biris, I. Misan, A. Jianu, G. Helzhuter and E. Burkel, *Int. J. Hydrogen Energy* **29**, 97 (2004).
24. J. Hedberg, J. Jiao, V. Dubin, J. Dominguez and R. Chebiam, *Microsc. Microanal.* **10 (Suppl. 2)**, 394 2004).
25. J. H. Han, S. H. Choi, T. Y. Lee, J. B. Yoo, C. Y. Park, T. Jung, S. Yu, W. Yi, I. T. Han and J. M. Kim, *Diamond Rel. Mater.* **12**, 878 (2003).
26. J. F. AuBuchon, L.-H. Chen, C. Daraio, A. Gapin and S.-H. Jin, *Nano Lett.* **6**, 324 (2006).
27. J. F. AuBuchon, L.-H. Chen, A. I. Gapin and S.-H. Jin, *Chemical Vapor Deposition* **12**, 370 (2006).